THE ASTROPHYSICAL JOURNAL, 447:L77–L80, 1995 July 10

EXTRAGALACTIC IONIZED HYDROGEN IN THE FORNAX CLUSTER

J. BLAND-HAWTHORN
Anglo-Australian Observatory, P.O. Box 296, Epping, NSW 2121, Australia

R. D. EKERS
Australia Telescope National Facility, P.O. Box 76, Epping, NSW 2121, Australia

W. VAN BREUGEL
Institute of Geophysics and Planetary Physics, Lawrence Livermore National Laboratory, P.O. Box 808, L-413, Livermore, CA 94551-9900

A. KOEKEMOER
Mount Stromlo and Siding Springs Observatories, The Australian National University, Private Bag, Weston Creek P.O., ACT 2611, Australia

AND

K. TAYLOR
Anglo-Australian Observatory, P.O. Box 296, Epping, NSW 2121, Australia
Received 1995 March 20; accepted 1995 May 2

ABSTRACT

The radio galaxy Fornax A is well known for its giant radio lobes which extend almost a degree (~300 kpc) across the sky. Fomalont et al. have shown that these lobes are linearly polarized on the largest scales, although the western lobe is highly depolarized in discrete, resolved regions. The depolarized regions indicate the presence of ionized gas (Faraday screen) along the line of sight to the western lobe. We have now detected the warm gas at Hα using a Fabry-Perot interferometer in a way that allows us to reach very low surface brightness levels ($<10^{-19}$ erg cm^{-2} s^{-1} arcsec^{-2}). The radial velocity of the ionized gas (1610 km s^{-1}) places it in the Fornax cluster at a projected radius of 1.0 Mpc. The gas is spread over a region 10 kpc in diameter and has an ionized mass of $6 \times 10^7 f^{-0.5} M_\odot$ (where f is the volume filling factor). For the inferred column density of electrons ($\approx 2.6 \times 10^{20} f^{-0.5}$ cm^{-2}) and in light of the H I upper limits ($<4 \times 10^{19}$ cm^{-2}), the cloud has to be mostly ionized. Possible sources of ionization are large-scale shocks or a putative hot component which confines the radio lobes. The high line-of-sight magnetic field strength ($B_\parallel \approx 0.3$–1.3 μG) deduced from the rotation measure (≈ 20 rad m^{-2}) and energy equipartition suggests that the cloud may have undergone significant turbulent heating from secondary shocks. The predicted bounds on the fraction of neutral material (10^{-6}–10^{-1}) indicates that this may be the first example of a spatially resolved, extragalactic ionized cloud. Such objects are thought to be responsible for some of the Lyα absorption lines observed in the spectra of quasars.

Subject headings: intergalactic medium — quasars: absorption lines — techniques: interferometric — techniques: spectroscopic

1. INTRODUCTION

Lyα forest lines in the spectra of distant quasars reveal that there exist gas clouds at large distances (>100 kpc) from galaxies. The trace amounts of neutral hydrogen, with column densities in the range 10^{13}–10^{17} cm^{-2}, presumably arise from gaseous structures that are almost fully ionized (see Sargent & Steidel 1990). The *Hubble Space Telescope* has now detected substantial numbers of Lyα clouds at low redshift toward 3C 273 (Bahcall et al. 1991; Morris et al. 1991) which has spurred efforts to observe one of these objects directly in optical line emission (Williams & Schommer 1993; Bland-Hawthorn et al. 1994; Vogel et al. 1995). The optical experiments have proved unsuccessful to date which has motivated us to consider alternative avenues. Rather than attempting blind searches for extragalactic ionized gas (e.g., Hogan & Weymann 1987), we have begun an optical survey of depolarized regions towards radio lobes with the specific aim of detecting warm gas along the line of sight. In this Letter, we describe our first results.

2. OBSERVATIONS

A small field in the western lobe of Fornax A (Fig. 1 [Pl. L11]) was observed on the dark nights of 1994 October 28–30 using TAURUS-2 at the f/8 and f/15 Cassegrain foci of the 3.9 m Anglo-Australian Telescope. A 40 μm Queensgate etalon was used at a high order of interference ($m = 75$) with a 45 Å blocking filter centered at 6594 Å. The etalon was used at fixed gap spacings and the resulting ring pattern was imaged onto a Tek 1024^2 CCD (read noise $\approx 2.3e^-$). The etalon free spectral range and instrumental resolution were measured to be 54.3 and 1.1 Å, respectively at Hα. We went to great lengths to suppress internal reflections within the system. The etalon was tilted to place the optical axis at the edge of the field (see Fig. 2 [Pl. L12]). The depolarized region was observed at two etalon settings (5 minutes, 20 minutes) at f/8 and three settings (20 minutes, 40 minutes, 100 minutes) at f/15, where the combined integration times are given in parentheses. An off-field position was observed for 60 minutes at f/15 at the same airmass as the longest combined integration. Flux cali-

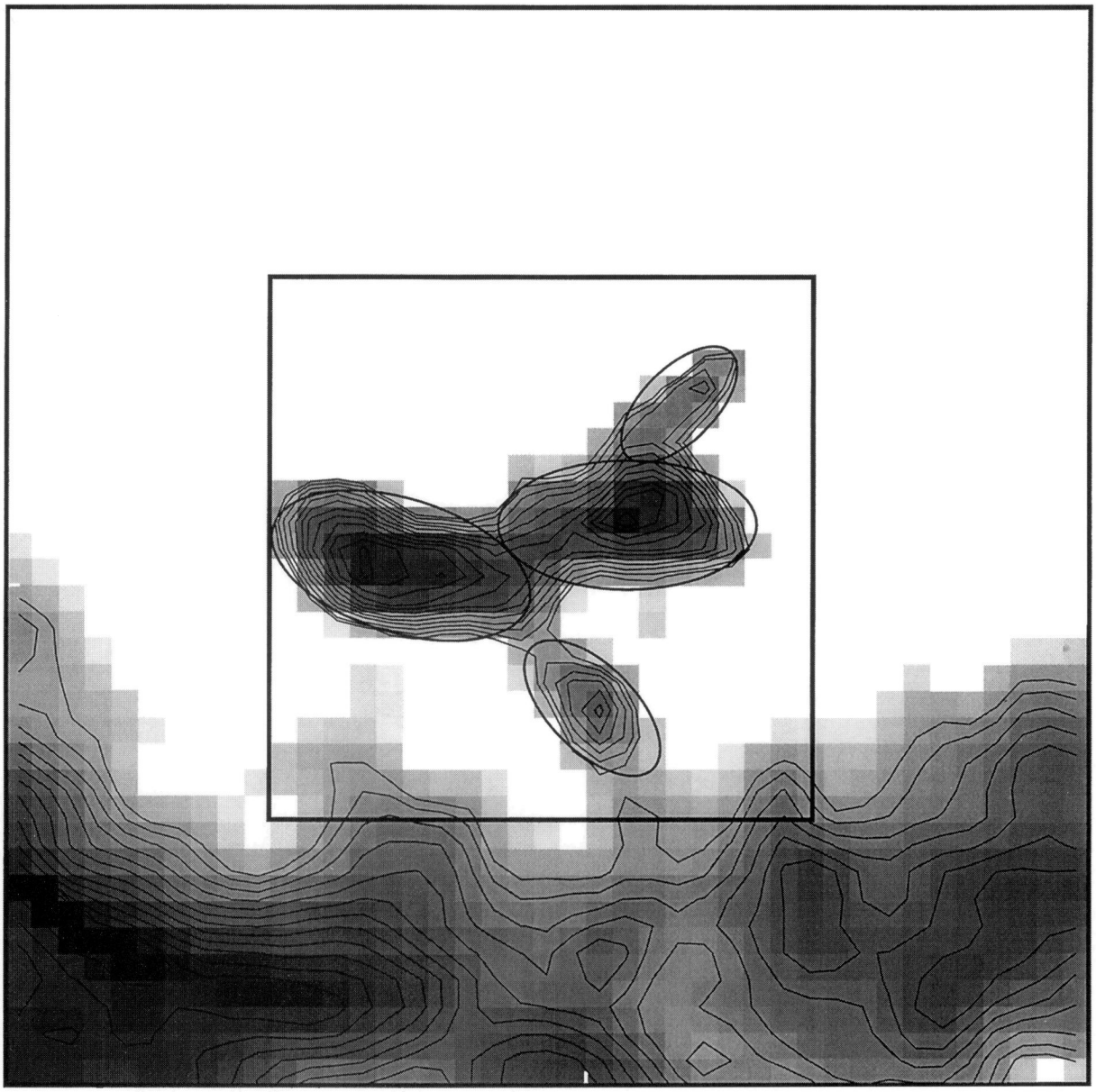

FIG. 1.—Percentage of linear polarization at 1.5 GHz over the "ant" region in Fornax A (FEBE) where north is at the top and east is to the left. The contrast of the image is linear between 5% (*black*) and 40% (*white*). The depolarized emission along the southern boundary arises from warm gas intrinsic to the lobe. The f/15 TAURUS-2 field of view (2′.4) is indicated by the inner box. The ellipses illustrate our model for the clumps (see text).

BLAND-HAWTHORN et al. (See 447, L77)

1995ApJ...447L..77B

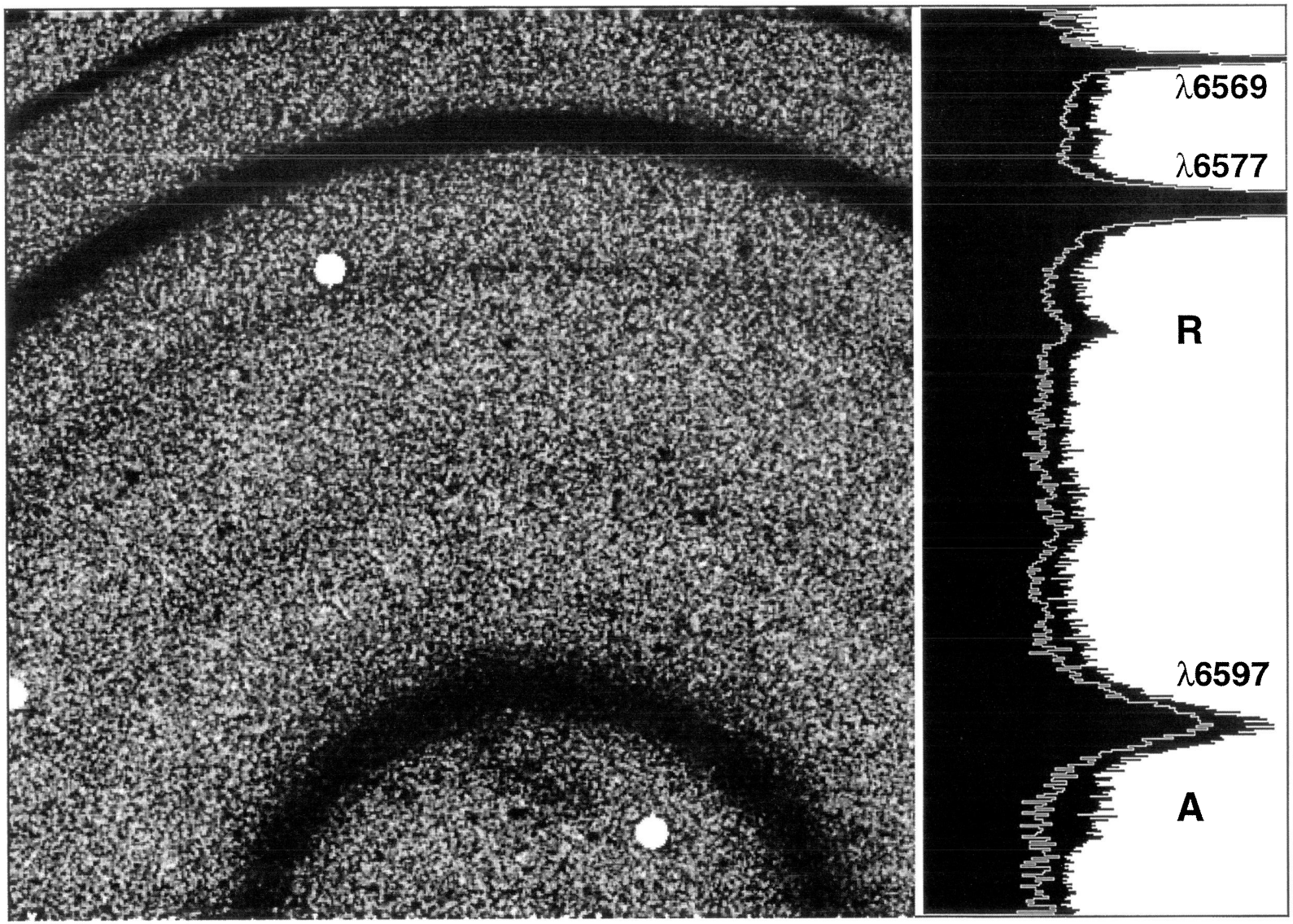

FIG. 2.—Deep observation at a fixed etalon gap with the TAURUS-2 Fabry-Perot interferometer from combining three exposures to give a total integration time of 100 minutes. After summing in annuli about the optical axis, we obtain the spectral trace shown in silhouette on the right. The white curve is the spectrum one gets from observing a blank field. In the main image, the white circles are stars which have been masked out. We have also removed bright cosmic-ray events. The field of view is 2.'4 and the spectral coverage (*top to bottom*) is λλ6562–6599. The three brightest features in the spectral trace are the atmospheric OH lines. The faint feature labeled "R" is [N II] λ6583 emission from the Reynolds layer of the Milky Way. The Hα detection of the 'ant' (labeled "A") falls on the wing of the red OH feature. This can also be seen in the direct image as a faint smudge covering 120 arcsec^2 below the bottom ring. The emission coincides with the southern extension of the "ant" in Fig. 1.

bration was performed with respect to two standard stars, Feige 110 and L870-2, and a planetary nebula, NGC 2438. A neon lamp was used to monitor the stability of the system.

3. THE SEARCH

The depolarized regions toward the western radio lobe of Fornax A were first seen by Fomalont et al. (1989, hereafter FEBE) in high resolution (14″) observations at 20 cm with the Very Large Array (VLA). One of these regions exhibits a highly elliptic shape and was subsequently shown to coincide with the optical disk of the foreground galaxy, NGC 1310 (Schulman & Fomalont 1992). Another of these, the "antlike feature" in the vernacular of FEBE, was puzzling particularly since deep searches at optical and radio wavelengths failed to find an obvious explanation. After stacking six IIIa-J Schmidt plates, D. F. Malin (1994, personal communication) has set an approximate upper limit of $B \approx 27.5$ mag arcsec^{-2} within the depolarized region. At 21 cm, J. van Gorkom (1994, personal communication) obtained an upper limit of 4×10^{19} cm^{-2} for the neutral hydrogen column.

We have used a novel technique to ascertain the radial velocity of the Faraday screen of warm gas (e.g., Burn 1966) giving rise to the depolarized silhouette. A rough calculation showed that the expected Hα surface brightness could be reached by a Fabry-Perot interferometer after coadding long exposures at a fixed etalon spacing (Bland-Hawthorn et al. 1994). The etalon cavity (optical gap = μd) disperses according to $m\lambda = 2\mu d \cos\theta$, where θ is the off-axis angle of an incoming ray with wavelength λ. The resulting small wavelength segment (≈40 Å) has a quadratic dispersion across the field with blue wavelengths farthest from the optical axis (see Fig. 2). The spectral coverage and the field of view at f/15 (2.′4) are ideally matched to both the size of the "ant" region (see Fig. 1) and the necessary velocity range to reach the far side of the Fornax cluster (1800 km s^{-1}).

4. THE DETECTION

In Figure 2, the bright ring sections are due to the atmospheric OH lines. The faint ring above the centre of the field is [N II] λ6583 emission from the warm ionized medium in the Milky Way (Reynolds 1984, 1992). For a nominal ratio of [N II]/H$\alpha \approx 0.3$, the [N II] line has an emission measure ~0.6 cm^{-6} pc, characteristic of the warm ionized medium at high ($b \approx -60°$) Galactic latitudes (Reynolds 1990). The Hα detection of the "ant" region coincides with the southernmost extension of the depolarized region in Fig. 1. To rule out the possibility that the line is blueshifted [N II] λ6583, we tilted the filter and took a 40 minute combined exposure at the expected position of Hα. No such feature was detected nor, for that matter, at the off-field position 5° to the south (see Fig. 2). The [N II] λ6548 line would need to be redshifted to 2300 km s^{-1} thereby placing the warm gas well beyond the radio lobes.

The observed Hα emission measure ($= \int n_e^2\, dl$, where l is the column depth through the cloud) was measured to be $E_m \approx 0.53$ cm^{-6} pc at 12 σ over an aperture of 10″ × 20″. This is equivalent to a line surface brightness of 4.7×10^{-8} erg cm^{-2} s^{-1} sr^{-1} (or 0.20 rayleighs). The line is centered at 1610 km s^{-1} as compared with 1770 km s^{-1} for NGC 1316 (Fornax A) and 1710 km s^{-1} for NGC 1310. The line flux has an intrinsic spread of 50 km s^{-1} and therefore the emission may be spectrally unresolved. An additional constraint would come from a simultaneous detection of the [N II] λ6548 line which is expected to be a factor of 4–12 times fainter than the Hα line. Unfortunately, at the redshift measured from the Hα line, this falls on the [N II] λ6583 line emission from the Milky Way. While it could be argued that the on-source emission is somewhat stronger than the off-source emission, the degree of uniformity within the Reynolds layer is not currently known.

5. CLOUD PARAMETERS

FEBE approximated the depolarized region as a sphere with diameter 10 kpc. But since the region clearly exhibits structure, we prefer to model the depolarized region as four distinct ellipsoids (or clumps) with diameters 6.0, 6.0, 4.0, and 3.3 kpc (see Fig. 1). We propose two limiting cases: prolate clumps with axis ratios 2:1:1 where the long axis lies in the plane of the sky, and oblate clumps with axis ratios 2:2:1 where the short axis is in the plane of the sky. The total volume of these clouds is then either 70 kpc^3 (prolate) or 140 kpc^3 (oblate) with a mean column depth, l, of either 2.4 kpc (prolate) or 4.8 kpc (oblate). Since we are only detecting a small part of the "ant" cloud, we have scaled the observed Hα emission measure ($E_m \approx f\langle n_e^2\rangle l$) to account for the variation in rotation measure over the object. Under the assumption that $B_\parallel$ is everywhere constant, this leads to a factor of 2 increase in E_m. To simplify matters, we adopt a triaxial shape for the clumps (2:1.5:1) with a mean depth $l \approx 3.6$ kpc for which the inferred average density is $\langle n_e\rangle = 0.025\, f^{-0.5}$ cm^{-3}.

We define the electron column density (or equivalently, the dispersion measure) as $N_e = \int n_e\, dl \approx 2.6 \times 10^{20}\, f^{-0.5}$ cm^{-2}. This is significantly larger than the upper limit on the neutral column density set by the VLA observations. For our simple model, the total mass in the four clumps is $6 \times 10^7\, f^{-0.5}\, M_\odot$. FEBE argue that the warm gas must have a turbulent cell size significantly smaller than the VLA beam size (≈1.2 kpc) in order to produce a rotation measure, $R_m = \int n_e B_\parallel\, dl \approx 20$ rad m^{-2}. Combined with our estimate of the local gas density, the average magnetic field strength along the line of sight, $B_\parallel$, is expected to fall in the range $0.3–0.9\, f^{0.5}$ μG. This compares with the energy equipartition field strength, $\sqrt{16\pi m_e k T_e} \approx 1.3\, f^{-0.25}$ μG, for an electron temperature of $T_e = 10^4$ K. Taken together, these independent, albeit crude, estimates of the field strength argue for a large filling factor.

For an ionized cloud of radius R, the necessary binding mass $5RkT_e(Gm_{\rm H})^{-1} \approx 10^8\, M_\odot$ suggests that the clouds may be marginally unbound, particularly in light of the inferred magnetic field strength. Since the clumps would otherwise evaporate in a sound crossing time (~10^8 yr), they may be confined by the external X-ray gas associated with the Fornax cluster and the general environs of Fornax A. The cluster gas temperature $T_{\rm X}$ is one of the lowest measured to date ($kT_{\rm X} = 1.2$ keV) presumably as a consequence of high metal enrichment (Ikebe et al. 1992). The X-ray density required to confine the cloud, $n_{\rm X} \approx 10^{-5}$ cm^{-3}, produces an X-ray emission measure more than a factor of 10 below the limits set by the *ROSAT* data (Feigelson et al. 1995). Other possibilities do exist, in particular, ram pressure confinement in large-scale shocks which we discuss below.

6. SOURCE OF IONIZATION

The recombination time within the cloud is only $(\alpha_T n_e)^{-1} \approx 9 \times 10^6\, f^{0.5}$ yr, where we have adopted a total recombination coefficient α_T (Case B) that reflects the high electron column (Osterbrock 1989). This raises the important

question as to what keeps the cloud highly ionized. The radiation field from the Fornax cluster (including both UV from the stellar population and X-rays from the hot gas) fails by at least an order of magnitude. Moreover, the known X-rays in the radio lobes from inverse Compton upscattering of the microwave background (Feigelson et al. 1995) also fail by the same margin. We note that the "ant" cloud falls along the radio axis from Fornax A at a projected distance of 90 kpc. If the cloud happens to lie at the same distance as the Fornax A nucleus, the observed nuclear X-ray source (Feigelson et al. 1995) would need to be at least ten times more luminous along the radio axis to account for the cloud ionization. An interesting possibility is the existence of a diffuse X-ray halo around Fornax A which is sufficiently hot to be undetectable by the *ROSAT* X-ray satellite. In principle, this hot gas could confine the radio lobes and ionize the "ant" cloud.

As a rough guideline to the required ionizing flux, we have performed a one-dimensional calculation along a line which passes through the centre of a gas cloud ionized at both ends. (As far as the authors have been able to establish, the general ionization problem of a spheroidal cloud embedded in a radiation bath has not been solved numerically.) In order to determine the external ionizing flux level that would keep the cloud fully ionized, we shall assume ionization balance such that

$$\int_{\nu_0}^{\infty} \frac{4\pi J_\nu}{h\nu}\, d\nu = 2\alpha_B \int_0^{\tau_c} n_e n_p dr, \qquad (1)$$

where the integration is performed from the centre to the edge r_c of the cloud. The quantity J_ν is the metagalactic flux which we shall express as

$$J_\nu = 10^{-21} J_{-21} \left(\frac{\nu_0}{\nu}\right)^{1.5}, \qquad (2)$$

where ν_0 is the Lyman limit frequency and J_{-21} is the metagalactic flux in units of 10^{-21} erg cm^{-2} s^{-1} Hz^{-1} sr^{-1}.

If we assume that the clumps are self-gravitating and in pure hydrostatic balance, the modified isothermal profile (Salucci & Frenck 1989) will be a reasonable approximation for which $n(r) = n_I/[1 + (r/r_s)^2]$. Moreover, if we assume that the cut-off radius r_c corresponds to the size of the observed cloud (suggested by the dramatic edge in the polarization map), we get a relation between r_c and r_s from the electron column density. Since

$$N_e = 2 \int_0^{r_c} \frac{n_I}{1 + (r/r_s)^2}\, dr, \qquad (3)$$

if we take the density at the origin to be $n_I = 2\langle n_e\rangle$, it follows that $r_c = 2.33 r_s$. Thus, we find $J_{-21} \approx 2\text{–}3\, f^{-1}$, which is a factor of 20–30 larger than the best upper limit ($J_{-21} < 0.1$; Vogel et al. 1995) for the metagalactic flux level at the present epoch (see Henry 1991; Bowyer 1991). A pressure-confined, constant density model for the clumps gives essentially the same result. A small filling factor requires an even higher flux level to ionize the cloud.

7. SHOCK HEATING

Without the detection of other spectral lines, it is difficult to set reliable limits on possible shock heating. However, we now demonstrate that large-scale shocks could go a long way toward explaining many aspects of the "ant" region, not least the clumpy structure observed in the depolarization data. When a strong shock occurs, there are three important zones to consider: (1) the preshock region (density n_0), (2) the postshock cooling region immediately behind the shock, (density n_1, temperature T_1), and (3) the post-shock radiative region (density n_2, temperature T_2). The cooling regions are expected to undergo large-scale fragmentation, either through Rayleigh-Taylor or through cooling instabilities. The observed average density $\langle n_e\rangle$ is then a flux-weighted average of n_0 and n_2.

M. A. Dopita has performed calculations with the newly revised MAPPINGS-II code (Sutherland & Dopita 1993) and has shown that the shock speed (v_s) internal to the cloud would have to be at least 400 km s^{-1} in order to generate the observed electron column N_e. We shall assume here that the metagalactic field plays no part in the ionization. If we take the characteristic dimension of the depolarized clumps (5 kpc) to be a cooling length l_c, we find $n_0 \sim 1.5 \times 10^{19} l_c^{-1} \sim 10^{-3}$ cm^{-3}. The constant arises from integrating the cooling function through the shock region. Since the pressure driven into the cloud should balance the ram pressure exerted by the ambient medium (density n_A), this leads to a rough estimate of the initial cloud velocity v_0 through the medium. If we take $n_A \sim 10^{-4}$ cm^{-3} (consistent with the upper limit set by *ROSAT*), we find $v_0 \sim v_s\sqrt{n_0/n_A} \sim 1300$ km s^{-1}.

The postshock temperature, $T_1 \sim 2.6 \times 10^6 (v_s/400)^2$ K, will produce mostly hard UV radiation with very little in the *ROSAT* (0.2–2.4 keV) bandpass. For the deduced B field and pre-shock density, MAPPINGS-II shows that the compression factor (n_2/n_0) is unlikely to exceed 75, therefore suggesting $n_2 \sim 0.1$ cm^{-3}. The postshock column of initially neutral hydrogen is expected to absorb of most of the downstream UV radiation produced by the shock. The cooling time of the shock is $\tau_c \sim 2.5 \times 10^{12} n_0^{-1} \sim 10^8$ yr. The predicted Hα surface brightness, $\Sigma_{H\alpha}$, is given by $\log \Sigma_{H\alpha} = 2.384 \log v_s + \log n_0 - 10.52$. The predicted value $\Sigma_{H\alpha} \approx 5 \times 10^{-8}$ erg cm^{-2} s^{-1} sr^{-1} agrees remarkably well with the observed surface brightness for our canonical values of v_s and n_0.

NGC 1310 lies 5′ (~25 kpc) due west of the "ant" complex and, as we have noted, is also seen in silhouette against the western lobe (Schulman & Fomalont 1992). One interesting possibility is that the depolarizing clumps are bound to NGC 1310 and are now visible after being hit by the wind associated with the radio lobes. If the leading surface of the lobe is moving at 1000 km s^{-1}, for a lobe electron density of 10^{-3} cm^{-3} (Feigelson et al. 1995), there could be sufficient shock pressure to explain the ionization of the "ant." This would require the "ant" region to be slightly embedded in the radio lobes. (We note in passing that the same lobe model could generate a visible galaxy-sized bow shock in the outer low density [$<10^{-2}$ cm^{-3}] regions of NGC 1310.) Another possible explanation is that the clumps are tidal debris from previous galaxy encounters. In this picture, the shock is due to the motion of the clumps through the cluster medium. Since there must be cell structure within the clumps to account for the depolarized signal, this could arise from turbulence driven by secondary shocks. These shocks will increase the internal B field until it is sufficiently rigid to damp out turbulence, at which point the Alfvén speed is of order the thermal sound speed. This is not expected to occur until $B \approx 2\text{–}3$ μG.

8. QUASAR SIGHT LINES

The *ROSAT* image described by Feigelson et al. (1995) contains several candidate sources with hard X-ray spectra within a few arcminutes of the depolarized region. While these may provide sight lines to high-redshift quasars, the optical candidates are too faint ($m_B > 20$) to provide decent Lyα absorption line spectra with the *Hubble Space Telescope.* Be that as it may, it is interesting to ask just what absorption line columns might be expected through the depolarized region. The column depth of neutral atoms ($N_{\rm H}$) through the cloud will depend on the ionization fraction ($x = n_e/n$) within the cloud, where n is the total number of atomic nuclei. This ratio depends sensitively on the source of ionization and the radiative transport through the cloud. Most detailed calculations to date consider one-dimensional radiative transport through a slab of gas (e.g., Donahue & Shull 1991). The results of these models are often characterized by the ionization parameter $U = J/(cn)$, or the ratio of photons to atomic nuclei at the front of the slab. For the power-law radiation field considered above, U probably lies in the range 10^{-4}–10^{-2} if the cloud is in ionization balance. However, shock ionization could increase U by 1 or 2 orders of magnitude. Thus, the hydrogen column density of a Lyα absorption line, $N_{\rm H} \approx (1 - x)\, N_e$, is expected to lie in the range 10^{14-19} cm^{-2} (see Donahue & Shull 1991, Fig. 5). This range is particularly interesting in light of recent observations with the *Hubble Space Telescope* which have revealed a surprisingly large population of Lyα absorption-line clouds at low redshift (Bahcall et al. 1991; Morris et al. 1991).

The relatively high emission measure in the southern extension (Fig. 2) indicates that it should be possible to detect the main body of the "ant" in the diagnostic lines [O II] λ3727, [O III] λ5007, [O I] λ6300, [N II] λ6583 and [S III] λ9532, depending of course on the source of ionization. Thus, in future observations, we anticipate setting strong constraints on U and, therefore, establishing whether we have found a candidate for a Lyα forest cloud, or at least part of a larger structure giving rise to Lyα forest lines.

In closing, it is interesting to consider whether low column-density plasmas are more easily detected from rotation measures at radio wavelengths against a polarized source, or from emission measures due to recombination at optical wavelengths. Bland-Hawthorn et al. (1994) are able to reach Hα emission measures of 0.02 cm^{-6} pc (3 σ) in a single night of observing. At radio wavelengths, the position angle variation χ (in radians) due to a magneto-ionic medium is given by $\chi(\lambda) = \chi(0) + \lambda^2 R_m$, where λ is traditionally in units of meters. At 20 cm, it should be possible to detect an incremental change of 0.1 rad, so that the limit in R_m is 2.5 rad m^{-2}. If it was possible to determine reliable position angles at 90 cm, this limit could be reduced to 0.2 rad m^{-2}. Thus, the ratio of the sensitivity limits of E_m to R_m is approximately $0.1(n_e/B_\parallel)$. Given that faint plasmas generally have low n_e, this ratio favors emission measure detections of diffuse gas by more than a factor of 10. Furthermore, emission measure detections do not require a background source and, therefore, can be searched for over a much larger fraction of sky.

J. B. H. would like to thank the VLA staff in New Mexico, particularly W. M. Goss and R. A. Perley, for their hospitality in the early stages of this work. R. J. Reynolds and P. L. Shopbell provided valuable criticisms on an early manuscript and an anonymous referee made a number of very useful suggestions. We would like to thank R. D. Cannon, Director of the AAO, for his continued support of the TAURUS-2 program. We are indebted to E. D. Feigelson, who supplied estimates of the X-ray flux toward Fornax A in advance of publication. M. A. Dopita kindly supplied the results of shock calculations in the presence of a magnetic field, once again in advance of publication. The etalon for these observations was graciously loaned to us by R. B. Tully of the University of Hawaii.

REFERENCES

Bahcall, J. N., et al. 1991, ApJ, 377, L5
Bland-Hawthorn, J., Taylor, K., Veilleux, S., & Shopbell, P. L. 1994, ApJ, 437, L95
Bowyer, S. 1991, ARA&A, 29, 59
Burn, B. J. 1966, MNRAS, 133, 67
Donahue, M., & Shull, J. M. 1991, ApJ, 383, 511
Feigelson, E. D., Laurent-Muehleisen, S. A., Kollgaard, R. I., & Fomalont, E. B. 1995, ApJ, submitted
Fomalont, E. B., Ebneter, K. A., van Breugel, W. J. M., & Ekers, R. D. 1989, ApJ, 346, L17 (FEBE)
Henry, R. C. 1991, ARA&A, 29, 89
Hogan, C. J., & Weymann, R. J. 1987, MNRAS, 225, 1P
Ikebe, Y., et al. 1992, ApJ, 384, L5
Morris, S. L., et al. 1991, ApJ, 377, L21
Osterbrock, D. E. 1989, Astrophysics of Gaseous Nebulae & Active Galactic Nuclei (Singapore: University Science Books)
Reynolds, R. J. 1984, ApJ, 282, 191
———. 1990, in Galactic & Extragalactic Background Radiation, ed. S. Bowyer & C. Leinert (Dordrecht: Kluwer), 157
———. 1992, ApJ, 392, L53
Salucci, P., & Frenck, C. S. 1989, MNRAS, 237, 247
Sargent, W. L. W., & Steidel, C. C. 1990, in Baryonic Dark Matter, ed. D. Lynden-Bell & G. Gilmore (Dordrecht: Kluwer), 223
Schulman, E., & Fomalont, E. B. 1992, AJ, 103, 1138
Sutherland, R. S., & Dopita, M. A. 1993, ApJS, 88, 253
Vogel, S. N., Weymann, R., Rauch, M., & Hamilton, T. 1995, ApJ, 441, 162
Williams, T. B., & Schommer, R. 1993, ApJ, 419, L53